



# SYNTHESIS AND CHARACTERIZATION OF LOW-DIMENSIONAL TEMPLATES: FUNCTIONALIZED GOLD NANO-PARTICLES (AU-NPs) DISPERSED IN ROOM TEMPERATURE NEMATIC LIQUID CRYSTALLINE DISPLAY MATERIAL

Akash Yadav<sup>1</sup>, Bharti Yadav<sup>1,2</sup>, B. S. Sharma<sup>3</sup>, Prashant Kumar Pandey<sup>4</sup>, Abhay S. Pandey<sup>5\*</sup>

## Abstract:

From the beginning of the last three decades, studies of the impact of nanomaterials on the characteristics of liquid crystals have piqued significant scientific interest. The ability to combine two entirely unrelated sciences into one new, cross-disciplinary subject of soft matter and nanostructure is made possible by the nano size. N-(biphenyl-4-yl)acetamide on reaction with n-pentoylchloride in presence of aluminum chloride gives N-(4'-pentanoylphenyl-4yl)acetamide, when treated with N<sub>2</sub>H<sub>4</sub> and KOH affords 1-(4'-aminophenyl-4-yl)pentan-1-one. This on further reaction with NaNO<sub>2</sub> and HCl at 0-5° C gives diazotized product 4'-pentylbiphenyl-4-diazoniumchloride. This product on working through Sandmeyer reaction affords 4'-pentylbiphenyl-4- carbonitrile which is also recognized as 4'-pentyl-4-cyanobiphenyl (5CB). This material is in a liquid crystalline form. Further, this material 5CB have been characterized and confirmed by various spectroscopic methods viz. <sup>1</sup>H-NMR and <sup>13</sup>C-NMR. Furthermore, low dimensional templates i.e. AuNPs were doped in the synthesized liquid crystalline material i.e. 5CB. Moreover, we made a report on an electro-optical and electrical study of gold nano particles (AuNPs), which are doped at single strength of 0.1 weight percent to nematic medium of the synthetic liquid crystal 5CB. Higher concentrations were not tested since it was found that AuNPs were bundled in various places at greater concentrations. The different electrical properties, including dielectric permittivity, loss, relaxation frequency, dielectric anisotropy and ionic conductivity, were measured using electrical (dielectric) spectroscopy for aligned samples that are homeotropic and planar in a frequency range of 1 Hz - 35 MHz. The nematic phase is what allows AuNPs to align from side to side to the nematic direction. Presence of AuNPs, on the other hand, improves nematic phase's local orientational arrangement of molecules. Because of this, the presence of AuNPs considerably reduces a threshold voltage required to switch an arrangement of the molecules as of a bright state i.e. planar arrangement toward dark state i.e. homeotropic arrangement.

**Keywords:** AuNPs, Nematic Displays, 5CB, <sup>1</sup>H-NMR, <sup>13</sup>C-NMR and Display Parameters.

<sup>1</sup>Ph.D. Research Scholar of Lords School of Sciences, Lords University, Chikani, Alwar, Rajasthan, India.

<sup>2</sup>Associate Professor of Physics, Government College, Kanina, Mahendergarh, Haryana, India.

<sup>3</sup>Professor and Pro-Chairperson of Lords University, Chikani, Alwar, Rajasthan, India.

<sup>4</sup>Professor of Physics and Director, Ansal Technical Campus, Lucknow, India.

<sup>5</sup>Associate Professor of Physics, Department of Science, Lucknow Public College of Professional Studies, Vinamra Khand, Gomti Nagar, Lucknow, India.

**\*Corresponding Author:** Dr. Abhay S. Pandey

Associate Professor of Physics, Department of Science, Lucknow Public College of Professional Studies, Vinamra Khand, Gomti Nagar, Lucknow, India. E-mail: abhaypandey.liquidcrystal@gmail.com

**DOI:** 10.48047/ecb/2023.12.si5a.0485

## 1. Introduction:

The impact developed by nanoparticles to the characteristics of liquid crystal is current and consistently sparks scientific curiosity [1]. In terms of the dimensional scale, billionth of a metre, or roughly single nanometer, it is said to be a mystical point. Due to alignment and anchoring of the liquid crystal, these nanoparticles and liquid crystals share inherent characteristics [2-6]. In certain investigations, nanoparticles have been utilized successfully to enhance the electro-optical qualities of materials used in liquid crystal displays [7-16]. Most of the time, nanoparticles decreased the threshold voltage ( $V_{th}$ ) necessary to transform the molecules' shape from planar to homeotropic [17]. The display properties (threshold voltage and dielectric anisotropy) of nematic liquid crystalline material at room temperature changed as a result of the doping of gold nanoparticles (Au-NPs), as reported in the current work. By combining the necessary quantity of Au-NPs and liquid crystal in anhydrous dichloromethane, the liquid crystal-nanoparticle composite has been created. The solution received a sonic treatment for duration of thirty minutes at room-temperature, after which solvent was secluded, additionally; the remedy was vacuum-dried. A microscope has been used to examine the homogeneous nano-composite's nature, and it is employed in this work as such. Basic display material 5CB, which is composed of nematic liquid crystalline material, has a nematic phase temperature range of 18-35 °C [18].

## 2. Synthesis and Characterization of a Room Temperature Liquid Crystalline Material 4'-pentyl-4-cyanobiphenyl (5CB):

### 2.1 Synthesis:

The chemical structure of the nematic liquid crystalline material 5CB having its low viscosity

and nematic phase temperature range of 18-35 °C is shown in **Figure 1**.

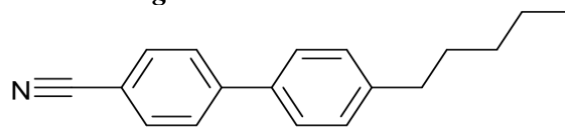


**Figure 1: Chemical structure of the synthesized nematic liquid crystalline material 5CB.**

CHEMICAL FORMULA:  $C_{18}H_{19}N$

Anal. Calcd: C =86.70%, H = 7.68 %, N = 5.62 %  
Found: C =86.68 %, H = 7.65 %, N = 5.59 %

N-(biphenyl-4-yl)acetamide on reaction with n-pentoylchloride in presence of aluminum chloride gives N-(4'-pentanoylphenyl-4-yl)acetamide, when treated with  $N_2H_4$  and KOH affords 1-(4'-aminophenyl-4-yl)pentan-1-one. This on further reaction with  $NaNO_2$  and HCl at 0-5° C gives diazotized product 4'-pentylbiphenyl-4-diazoniumchloride. This product on working through Sandmeyer reaction affords 4'-pentylbiphenyl-4- carbonitrile which is also known as 4'pentyl-4-cyanobiphenyl (5CB). This material is in a liquid crystalline form.

### 2.2 Characterization:

Carbon-13 ( $C_{13}$ ) nuclear magnetic resonance (most commonly known as carbon-13 NMR spectroscopy or  $^{13}C$  NMR spectroscopy or sometimes simply referred to as carbon NMR) is the application of nuclear magnetic resonance (NMR) spectroscopy to carbon. It is analogous to proton NMR ( $^1H$  NMR) and allows the identification of carbon atoms in an organic molecule just as proton NMR identifies hydrogen atoms.  $^{13}C$  NMR detects only the  $^{13}C$  isotope. The main carbon isotope,  $^{12}C$  is not detected. Although much less sensitive than  $^1H$  NMR spectroscopy,  $^{13}C$  NMR spectroscopy is widely used for characterizing organic and organometallic compounds.

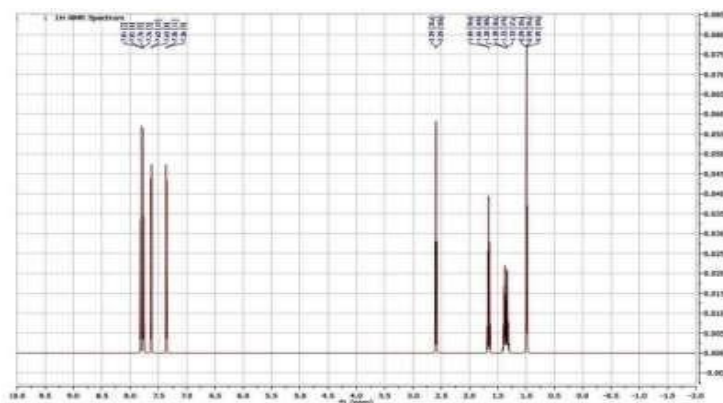


**Figure 2:  $^1H$  NMR Spectrum of the liquid crystalline substance 5CB demonstrates that the molecule was effectively synthesized.**

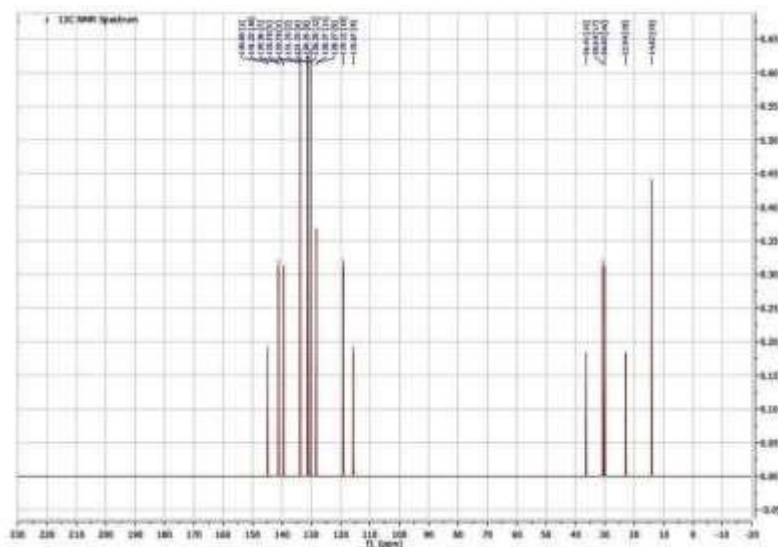


**Figure 3:**  $^{13}\text{C}$  NMR Spectrum of the liquid crystalline substance 5CB shows that the compound was synthesized successfully.

### 3. Experimental Methods used in Electrical and Electro-Optical Research:

Parallel-rubbed and polymer-coated Indium Tin Oxide (ITO) - coated pre-tilted glass plates at an angle of 1-3 were employed to create the cells with electrode spacing ( $d$ ) of  $5\ \mu\text{m}$  for research of the Electro-Optical (E-O) characteristics. These cells were bought from Instec in the United States. These cells have molecules that are in line with the direction that the glass plates are being rubbed. To determine the transverse component's static value of relative dielectric permittivity ( $\epsilon_{\perp}'$ ), the same cell was employed. Nevertheless, to create the cells needed for the longitudinal component measurement of relative dielectric permittivity ( $\epsilon_{\parallel}'$ ), glass plates with a gold coating and an extra lecithin coating were used. With the use of a polarised light microscope and an Instec photo-detector device, E-O characteristics, or curves for transmission voltage (T-V) were generated. The photo-voltage was measured using an Agilent multimeter with six and a half digits; this depends on the light's transmission's intensity, which was acquired from the photo-detector (model-34410A). The T-V curve was used to calculate  $V_{\text{th}}$ . Making use of the Newton's Phase-Sensitive Multimeter (model-1735) in conjunction with the Impedance Analysis Interface (IAI model-1257); dielectric data in the frequency range of 1 Hz to 35 MHz have been gathered in both planar and homeotropic anchoring of the molecules. A hot stage with precision of  $\pm 0.1^\circ\text{C}$  (Instec, model

HS-1) was applied to regulate the sample's temperature.

Using a common non-polar liquid (cyclohexane in this example), active capacitance ( $C_A$ ) of homeotropic cell was calculated using the formula:

$$C_A = [C(\text{ch}) - C(\text{a})] / [\epsilon'(\text{ch}) - 1], \quad (1)$$

Where  $\epsilon'(\text{ch})$  is the relative permittivity of cyclohexane and  $C(\text{ch})$  and  $C(\text{a})$  are the cell's capacitance when filled with cyclohexane or air, correspondingly. By measuring capacity of the cell when complete cyclohexane removal from the cell (after calibration) was ensured both before and after it was filled with cyclohexane.

The following equations have been used to compute the material's dielectric permittivity and loss:

In the case of a homeotropic aligned cell:

$$\epsilon' = [C(\text{m}) - C(\text{a})] / C_A + 1 \quad (2a)$$

In the case of a planar aligned cell:

$$\epsilon' = C(\text{m}) / (C_A = 34.0\text{pF}) \quad (2b)$$

and

$$\epsilon'' = 1/2 \pi f R C_A \quad (3)$$

where,  $\epsilon'$  and  $\epsilon''$  respectively, and represent the dielectric permittivity and loss;  $C(\text{m})$  is the material-filled capacitance of a cell,  $R$  is the material's resistance, and  $f$  is its frequency when it is encased between two parallel glass plates.

The generalized Cole-Cole equation is employable to characterise the dielectric spectrum that was noticed for dispersive materials [19, 20]:

$$\varepsilon^* = \varepsilon' - j\varepsilon'' = \varepsilon'(\infty) + \frac{\Delta\varepsilon}{1 + (jf\tau)^{1-h}} + \frac{A}{(f)^n} - j \frac{\sigma_{ion}}{2\pi\varepsilon_0 f^k} - jBf^m \quad (4)$$

where  $\varepsilon(0)$ -  $\varepsilon(\infty)$ ,  $\tau$  and  $h$  is the dielectric strength, the relaxation time (inverse of relaxation frequency) and the symmetric distribution parameter ( $0 < h < 1$ ) of the mode, respectively;  $\varepsilon(0)$  and  $\varepsilon(\infty)$ , the relative dielectric permittivity's limiting values at low and high frequencies; and the third and fourth terms in Equation (4), demonstrate the role played by the electrode polarisation capacitance and ionic conductance at

low frequencies where  $A$  and  $n$  are constants [21]. Constant  $k$  is found to be 1 for pure ohmic conductance. Equation (4) includes the fifth imaginary component  $Bf^m$  to partially account for the high-frequency electrode surface resistance [22, 23],  $B$  and  $m$  being constants as long as correction is small and  $\varepsilon_0$  ( $= 8.85 \text{ pFm}^{-1}$ ) is the free space permittivity.

Equation (4) may be written as follows for the real and imaginary parts:

$$\varepsilon' = \varepsilon'(\infty) + \frac{\Delta\varepsilon \left[ 1 + (f\tau)^{1-h} \sin\left(\frac{h\pi}{2}\right) \right]}{1 + (f\tau)^{2(1-h)} + 2(f\tau)^{(1-h)} \sin\left(\frac{h\pi}{2}\right)} + \frac{A}{f^n} \quad (5)$$

and

$$\varepsilon'' = \frac{\Delta\varepsilon (f\tau)^{(1-h)} \cos\left(\frac{h\pi}{2}\right)}{1 + (f\tau)^{2(1-h)} + 2(f\tau)^{(1-h)} \sin\left(\frac{h\pi}{2}\right)} + \frac{\sigma_{ion}}{2\pi\varepsilon_0 f^k} + Bf^m \quad (6)$$

Equations (5) and (6) have been used to fit the loss data and dielectric permittivity in order to examine the relaxation mode of the pure and dispersed systems. In order to investigate the relaxation process in nematic phase, we have eliminated low frequency correction components resulting from electrode polarisation capacitance from the obtained data. As there are no low- or high-frequency artifacts and up to this frequency, there was no dispersion mechanism, the 10 kHz dielectric information has considered as the "static" values [21, 23, 24]. These facts have been utilized to establish the anisotropy of the relative dielectric permittivity  $\Delta\varepsilon' (= \varepsilon'_{||} - \varepsilon'_{\perp})$ .

#### 4. Results and discussion:

At a single dose of 0.1% (weight ratio), AuNPs have been doped with 5CB. The homogeneous dispersion of AuNPs in the nematic framework of 5CB is confirmed by the optical texture of 5CB treated with 0.1 wt% AuNPs in the planar orientation seen in **Figure 4**. T-V trends for pure and AuNPs - doped 5CB samples at 20.0 °C are shown in **Figure 4**. When molecules are aligned in a planar manner at low voltages ( $< V_{th}$ ), a brilliant state is seen. Molecules eventually

change to a homeotropic orientation (molecular orientation normal to the surface of the electrode) as applied voltage is raised above  $V_{th}$ , and dark condition is seen.

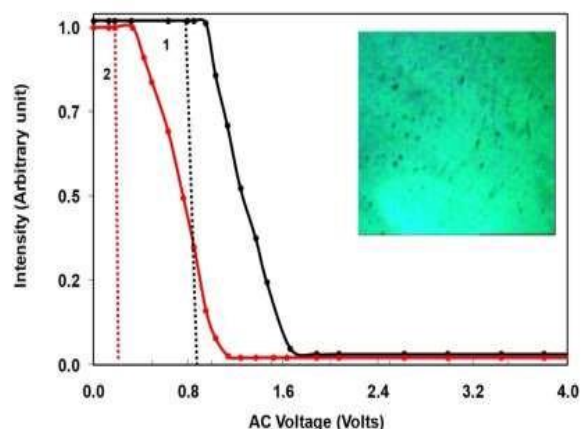


**Figure 4: Electro-optic sensitivity to the applied voltage at 1 kHz for the following two cell types: (1) pure 5CB liquid crystal cells, and (2) cells with 0.1 wt% gold nanoparticles dispersed in 5CB. Threshold voltages are shown by vertical lines. The brilliant condition of the cell containing 0.1 weight percent of gold nanoparticles distributed in 5CB is seen in the photomicrograph in the inset.**



Switching voltage interval is voltage needed to shift the intensity from 90% of the maximum value to 10%. The switch voltage interval serves as a gauge for the T-V curve's steepness. **Table 1** provides the threshold voltages derived from these T-V curves. It is evident from **Figure 4** and **Table 1** that when AuNPs are doped in nematic liquid crystals (NLC),  $V_{th}$  significantly reduces, which is desirable from an application standpoint. Low values of  $\Delta\epsilon'/\epsilon'_\perp$  ( $<1$ ) are preferred for low optical anisotropy materials to increase the gradient of the transmission voltage graphical curve. When it comes to the pure 5CB sample (at 23.0 °C),  $\epsilon'_{||} = 19.05$  and  $\epsilon'_\perp = 6.12$ ; i.e.  $\Delta\epsilon' = 12.93$  and  $\Delta\epsilon'/\epsilon'_\perp = 2.11$ . For AuNPs doped 5CB sample (at 23.0 °C),  $\epsilon'_{||} = 11.15$  and  $\epsilon'_\perp = 6.08$ ; i.e.  $\Delta\epsilon' = 5.07$  and  $\Delta\epsilon'/\epsilon'_\perp = 0.83$ . The above data suggest that the steepness of the T-V curve is also improving due to the doping of AuNPs (see **Table 1** and **Figure 4**). The equation governs the threshold voltage:

$$V_{th} = \pi \left( \frac{K_{11}}{\epsilon_0 \Delta\epsilon'} \right)^{1/2} \quad (7)$$

where  $K_{11}$  for twisted / parallel cells, respectively.  $K_{11}$  is the splay elastic constants and  $\epsilon_0$  ( $=8.85$  pF/m) is the free space permittivity.

**Figure 5** depicts variations in  $\epsilon'_{||}$  and  $\epsilon'_\perp$  (and hence  $\Delta\epsilon' (= \epsilon'_{||} - \epsilon'_\perp)$ ) with temperature intended for both pure and AuNPs doped 5CB samples. The Nematic - Isotropic Transition Temperature ( $T_{N-I}$ ), which is important for displaying purposes due to the large temperature array of the nematic phase, is shown to be enhanced by 3.3 °C for AuNPs doped samples in comparison to pure samples. This is because the liquid crystal molecules

become polarised in consequence of the nanoparticles' enormous local electric fields, which in turn increases intermolecular interactions.

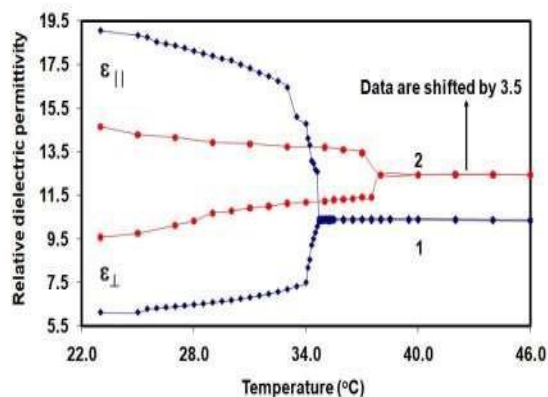


**Figure 5: The results for the nematic and isotropic phases of (1) pure 5CB compound and (2) 5CB with 0.1 wt% of gold nanoparticles distributed are moved by a quantity of 3.5 in relation to temperature for the real portion of dielectric permittivity in the heating cycle at 10 kHz (static value).**

A greater isotropic-nematic transition temperature results from this enhanced interaction [25]. This method has the drawback of not taking the orientational dispersion of the nanoparticles into account. He estimated the coupling strength and then assessed the subsequent improvement in  $T_{N-I}$ , in strong agreement with experiments [26]. According to one other paper, the orientational allocation of the nanoparticle dipole moments is characterised by a directional order parameter, which interferes with the directional order of the liquid crystals and stabilises the nematic phase. With doped samples, the dielectric anisotropy diminishes (see **Table 1**).

**Table 1. Threshold voltage ( $V_{th}$  at 1 kHz with AC field and at 23.0 °C), dielectric anisotropy ( $\Delta\epsilon'$  at 10 kHz and at 23.0 °C), value of the quantity  $\Delta\epsilon'/\epsilon'_\perp$  at 23.0 °C, ionic conductivity anisotropy (at 25.0 °C), clearing temperature ( $T_{N-I}$ ), activation energy ( $E_a$ ) for nematic phase and relaxation frequency ( $f_r$ ) corresponding to flip-flop motion of molecules about their short axes at 23.0 °C.**

Sample	$V_{th}$ (volts)	$\Delta\epsilon'/\epsilon'_\perp$	$\Delta\epsilon'$	$\Delta\sigma_{ionic} (Sm^{-1})$	$T_{N-I} (°C)$	$E_a$ (kJ/mole)	$f_r$ (MHz)
5CB Pure	0.85	2.11	12.93	$4.34 \times 10^{-7}$	34.7	80.5	3.8
AuNPs Doped 5CB	0.33	0.83	5.07	$3.46 \times 10^{-6}$	38.0	74.1	5.7

The Maier and Meier theory [27] claims:

$$\Delta\epsilon' = \frac{NHF}{\epsilon_0} \left[ \Delta\alpha - \frac{F}{2kT} \mu^2 (1 - 3\cos^2\beta) \right] S \quad (8)$$

According to Maier and Meier theory, the longitudinal and transverse components of the dielectric constant are given by:

$$\epsilon'_{||} = 1 + \frac{NHF}{\epsilon_0} \left\{ \alpha_{av} + \frac{2}{3} S \Delta \alpha + F g_{||} \frac{\mu^2}{3kT} [1 - (1 - 3 \cos^2 \beta) S] \right\} \quad (9)$$

$$\epsilon'_{\perp} = 1 + \frac{NHF}{\epsilon_0} \left\{ \alpha_{av} - \frac{1}{3} S \Delta \alpha + F g_{\perp} \frac{\mu^2}{3kT} \left[ 1 + \left( \frac{1}{2} - 3 \cos^2 \beta \right) S \right] \right\} \quad (10)$$

Equations (9) and (10) are simplified to get the isotropic phase's dielectric constant as:

$$\epsilon_{iso} = 1 + \frac{NHF}{\epsilon_0} \left\{ \alpha_{av} + F \frac{\mu^2}{3kT} \right\} \quad (11)$$

where N denotes the density of molecules, S the order parameter,  $\alpha_{av}$  the average polarisability,  $\Delta \alpha$  the average anisotropy of the polarisability,  $\mu$  the consequent dipole moment of the molecule, and  $\beta$  the angle between the dipole moment and the molecule's long axis and F the feedback factor and  $H = \left( \frac{3\epsilon(0)}{2\epsilon(0)+1} \right)$ . In this case,  $\Delta \epsilon'$  is proportional

to the macroscale parameters S and N (molecules of liquid crystals per unit volume). N should decline as a result of the doping of AuNPs, which is projected to happen.

The cell electrodes are made of gold-coated glass plates, we measured  $\epsilon'_{||}$  and  $\epsilon'_{\perp}$  as a function of frequency to determine the impact of AuNPs at the molecular level.  $\epsilon'_{\perp}$  has been shown to be virtually unchanged across the frequency range from 1 Hz to 10 MHz, suggesting that dielectric relaxation related to molecule rotation along their long axes occurs far above this frequency.  $\epsilon'_{||}$  reveals a relaxation mechanism in high frequency range, nevertheless (in **Figure 6**). We equate it to molecules flip-flopping around their short axes

according to the values of relaxation frequencies. The relaxation frequency increases when AuNPs are doped. Hence, by doping AuNPs, the frequency range that may be used (below the relaxation frequency) for display technology is expanded. Because of the inclusion of AuNPs in nematic matrix of 5CB, total number of 5CB molecules per unit volume will reduce and it will promote flip-flop motion of 5CB molecules along their short axes [28]. This increase in relaxation frequency results from overhead discussion. The relaxation frequency rises as a result of the molecules' flip-flop motion over their short axes. The relaxation frequencies are governed by Arrhenius' equation:

$$f_r = A \exp \left( \frac{-E_a}{N_A kT} \right) \quad (12)$$

Where  $E_a$  is the energy of activation corresponding to the flip-flop motion of molecules along their short axes,  $N_A$  is the Avagadro number and k is the Boltzman constant. The least squares fit approach has been used to get the inclinations of the  $\log(f_r)$  vs. inversion of temperature plots. Using the inclines of straight lines, the energy of activation ( $E_a$ ) has now been calculated for both pure and doped systems. (see **Table 1**). **Figure 7** illustrates how the electrical conductivity of pure NLC material and the composite of AuNPs changes in parallel and perpendicular directions with temperature.

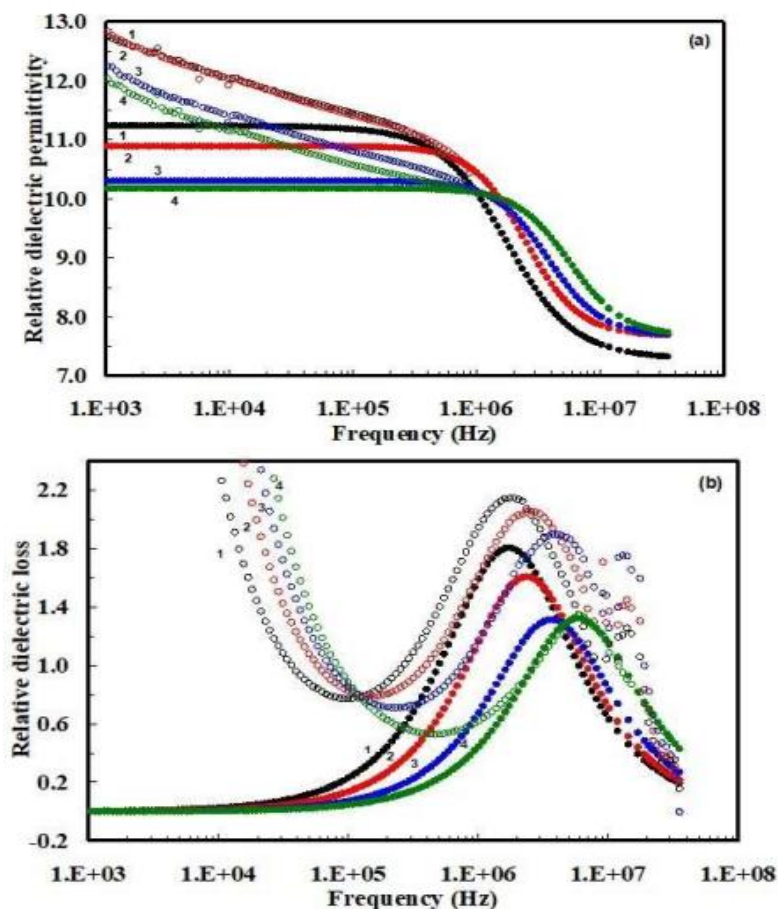


**Figure 6:** Frequency dependence of (a) relative dielectric permittivity and (b) loss in homeotropic aligned sample at temperatures 11.0 °C (1), 15.0 °C (2), 19.0 °C (3) and 23.0 °C (4) for 0.1 wt% of gold nano particles dispersed in 5CB. Hollow circles represent the raw experimental data, while filled circles data are data extracted by the process of fitting of equations (5) and (6).

As compared to pure 5CB, it is discovered that the electrical conductivity anisotropy rises by around 8 times (see *Table 1*). Anisotropy in electrical conductivity may be defined as  $\Delta\sigma = \sigma_{||} - \sigma_{\perp}$ .

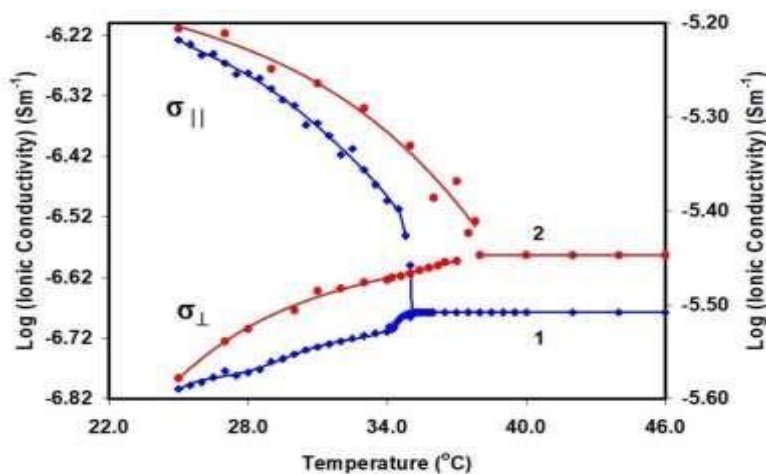


**Figure 7:** The temperature dependence of the ionic conductivity along parallel and perpendicular to the director of (1) the pure 5CB compound on primary axis and (2) 0.1 wt% of gold nano particles dispersed in 5CB on secondary axis.

Prasad et al. [29] research on 5CB- AuNPs composites at various concentrations revealed that

the system's electrical conductivity is increased by more than an order of magnitude (for the 5%

concentration of AuNPs) when AuNPs is present. AuNPs in 5CB had an impact on both electrical conductivity components. He proposed that the AuNPs functioned in the LC system like an ionic additive.

### 5. Conclusions:

The following points summarize the experimental results for pure, and with 0.1% GNPs or AuNPs in 5CB.

- The liquid crystalline material 4'-pentyl-4-cyanobiphenyl (5CB) have been synthesized at laboratory through standard operating procedure. It was separated out, dried and melting point was recorded on *Toshniwal Electronic Melting Point Apparatus*. Analysis was confirmed by calculating C, H, N, S via mass % of the sample. The  $^1\text{H}$  NMR and  $^{13}\text{C}$  NMR were recorded which confirms that the compound was successfully synthesized.
- Electrical (dielectric) spectroscopy for planar and homeotropic aligned samples has been carried out in the frequency range 1 Hz – 35 MHz and the various electrical parameters namely dielectric permittivity, loss, dielectric anisotropy, relaxation frequency, and ionic conductivity have been determined.
- It is originate that the nematic phase supports alignment of AuNPs parallel to the nematic director. On the other hand, the presence of AuNPs improves local orientational ordering of molecules in the nematic phase. Consequently, the threshold voltage required to switch the molecules from planar (bright state) to homeotropic (dark state) arrangement is considerably reduced in the existence of the AuNPs.
- The presence of AuNPs improves local orientational ordering of molecules in the nematic phase; and gets better result for the electrical conductivity and transition temperature.
- The relaxation frequency corresponding to the flip-flop motion of the molecules about their short axes increases. Thus usable frequency range (below relaxation frequency) for display applications increases for dispersed system.

### Acknowledgements:

The authors appreciate the professional guidance and comments provided by Prof. (Dr.) Ravindra Dhar, Head of the Materials Sciences Department at I. I. D. S. at the University of Allahabad in Prayagraj, on the experiments and data analysis.

### References:

1. H. Stark, Physics of colloidal dispersions in nematic liquid crystals, *Phys. Repts* **351** (2001), 387-474.
2. Yu. Reznikov, O. Buchnev, O. Tereshchenko, V. Reshetnyak, A. Glushchenko and J. West, *Applied Physics Letters*, 82(2003), 1917-1919.
3. J. Prakash, A. Choudhary, A. Kumar, D. S. Mehta, and A. M. Biradar, *Appl. Phys. Lett.* **93**(2008), 112904.
4. A. Kumar, J. Prakash, D. S. Mehta, A. M. Biradar, and W. Haase, *Appl. Phys. Lett.* **95**(2009), 023117.
5. J. Prakash, A. Choudhary, D. S. Mehta, and A. M. Biradar, *Phys. Rev. E* **80**(2009), 012701.
6. Neeraj and K. K. Raina, *Phase Transitions* **83**(2010), 615-626.
7. S. Kaur, S. P. Singh, A. M. Biradar, A. Choudhary, and K. Sreenivas: *Appl. Phys. Lett.* **91**(2007) 023120.
8. S. Kumar and H. Bisoyi: *Angew. Chem., Int. Ed.* **46** (2007) 1501.
9. S. Kumar, S.K. Pal, P. S. Kumar, V. Lakshminarayanan: *Soft Matter* **3** (2007) 896.
10. Y. Shiraishi, N. Toshima, K. Maeda, H. Yoshikawa, J. Xu, and S. Kobayashi: *Appl. Phys. Lett.* **81** (2002) 2845.
11. O. Buchnev, A. Dyadyusha, M. Kachmarek, V. Reshetnyak and Y. Reznikov: *J. Opt. Soc. Am. B* **24**(2007) 1512.
12. C. I. Cheon, L. Li, A. Glushchenko, J. L. West, Y. Reznikov, J. S. Kim, and D. H. Kim: *SID Int. Symp. Dig. Tech. Pap.* **36** (2005) 1471.
13. F. Haraguchi, K. Inoue, N. Toshima, S. Kobayashi, and K. Takotoh: *Jpn. J. Appl. Phys.* **34** (2007) L796.
14. A. Mikulko, P. Arora, A. Glushchenko, A. Lapanikand W. Haase: *EPL*, **87** (2009) 27009.
15. R. Dhar, S. N. Paul, S. Sharma and R. Dabrowski: Presented in ILCC, 2009, Poland.
16. S. N. Paul, R. Dhar, R. Verma, S. Sharma and R. Dabrowski: Presented in ILCC, 2010, Poland.
17. R. Dhar, A. S. Pandey, M. B. Pandey, S. Kumar and R. Dabrowski, *App. Phys. Exp.*, **1** (2008) 121501.
18. D. A. Dunmur, M. R. Manterfield, W. H. Miller and J. K. Dunleavy: *Mol. Cryst. Liq. Cryst.* **45**(1978) 127.
19. K.S. Cole and R.H. Cole: *J. Chem. Phys.* **9**(1941), 341.
20. M.B. Pandey, R. Dhar, V.K. Agrawal, R.P. Khare, and R. Dabrowski: *Phase Transitions* **76**(2003), 945.
21. S.L. Srivastava and R. Dhar: *Indian. J. Pure Appl. Phys.* **29**(1991), 745.



- 22.S.L. Srivastava: Proc. Natl. Acad. Sci. India 63(1993), 311.
- 23.R. Dhar: Indian J. Pure Appl. Phys. 42(2004), 56.
- 24.M. B. Pandey, R. Dhar, V. K. Agrawal, R. Dabrowski and M. Tykarska: Liq. Cryst. 31 (2004) 973.
- 25.Fenghua Li, OleksandrBuchnev, Chae Il Cheon, AnatoliyGlushchenko, Victor Reshetnyak, Yuri Reznikov, Timothy J. Sluckin, and John L. West: Phys. Rev. Lett. 97(2006), 147801; 99(2007), 219901(E).
- 26.Lena M. Lopatina and Jonathan V. Selinger:Phys. Rev. Lett. 102(2009), 197802.
- 27.W. Maier and G. Meier: Z. Naturforsch16A (1961) 262.
- 28.D.M.F. Edwards and P.A. Madden, Mol. Phys. 48, 471 (1983).
- 29.S. Krishna Prasad, K. L. Sandhya, Geetha G. Nair, Uma S. Hiremath, C. V. Yelamaggad, and S. Sampath: Liquid Crystals, 33(2006), 1121.